*Thermophysics and Aeromechanics*, *2017*, *Vol. 24*, *No. 1*

DOI: 10.1134/S0869864317010024

# Numerical simulation of nonequilibrium flows by using the state-to-state approach in commercial software*

**O.V. Kunova[1,2], G.V. Shoev[1,3], and A.N. Kudryavtsev[1,3]**

[1]*Novosibirsk State University*, *Novosibirsk*, *Russia*

[2]*St. Petersburg State University*, *St. Petersburg*, *Russia*

[3]*Khristianovich Institute of Theoretical and Applied Mechanics SB RAS*, *Novosibirsk*, *Russia*

E-mail: kunova.olga@gmail.com

(*Received January 12*, *2016*)

Nonequilibrium flows of a two-component oxygen mixture $O_2$/O behind a shock wave are studied with due allowance for the state-to-state vibrational and chemical kinetics. The system of gas-dynamic equations is supplemented with kinetic equations including contributions of VT (TV)-exchange and dissociation processes. A method of the numerical solution of this system with the use of the ANSYS Fluent commercial software package is proposed, which is used in a combination with the authors' code that takes into account nonequilibrium kinetics. The computed results are compared with parameters obtained by solving the problem in the shock-fitting formulation. The vibrational temperature is compared with experimental data. The numerical tool proposed in the present paper is applied to study the flow around a cylinder.

**Key words:** state-to-state kinetics, numerical simulation, nonequilibrium dissociation, vibrational relaxation, shock wave.

## Introduction

The processes of nonequilibrium vibrational and chemical kinetics are important aspects of studying flows behind shock waves formed near reentry vehicles, in nozzles, and in high-enthalpy facilities and combustion chambers. Under conditions of a significant deviation from the thermal equilibrium state, the characteristic times of kinetic processes become comparable with the times of variation of gas-dynamic parameters. Therefore, the kinetics of nonequilibrium processes should be considered together with gas-dynamic equations in modeling such flows.

Various approaches to the description of nonequilibrium flows of reacting gas mixtures for different degrees of deviation from the thermal and chemical equilibrium states were developed on the basis of the kinetic theory [1, 2]. The most detailed state-to-state approach describes vibrational relaxation and chemical reactions with retaining equilibrium or weakly nonequilibrium

* This work was supported by the Russian Foundation for Basic Research (Grant Nos. 15-31-51260 and 15-01-02373) and by the St. Petersburg State University (NIR 6.50.2522.2013).

distributions of velocities and vibrational energies. In this case, the characteristic times of relaxation satisfy the condition

$$\tau_{\text{tr}} \le \tau_{\text{rot}} << \tau_{\text{vibr}} < \tau_{\text{react}} \sim \theta, \tag{1}$$

where $\tau_{\text{tr}}$, $\tau_{\text{rot}}$, $\tau_{\text{vibr}}$, $\tau_{\text{react}}$, and $\theta$ are the relaxation times of translational, rotational, and vibrational degrees of freedom, chemical relaxation time, and mean time of variation of macroscopic parameters of the gas.

The state-to-state approach has been used in recent decades for numerical simulation of various flows, such as the flow behind the shock wave [3–6], in nozzles [7–9], in the boundary layer [10, 11], near the reentry vehicle surface [12, 13], etc. However, the majority of these investigations were aimed at studying steady inviscid gas flows or at estimating the effect of nonequilibrium kinetics on transport processes [6, 13] with the use of a simplified approach based on processing inviscid numerical solutions. The reason is that application of the state-to-state approach in the viscous formulation requires solving a large number of equations for populations of vibrational levels of molecular components of the mixture and number densities of atomic components. Moreover, the computational code should include expressions for calculating the rate coefficients of various processes and transport coefficients, which, in turn, depend on the vibrational level of molecules and flow macroparameters [14, 15]. In such a formulation, the problem computations are rather difficult.

The present paper describes the development of a computational tool, which would allow one to study two-dimensional and three-dimensional flows of reacting gas mixtures within the framework of the state-to-state approach and also to take into account the transport processes in subsequent computations. The solver was chosen to be the ANSYS Fluent software package, which was successfully used for numerical simulation of external [16] and internal [17] flows and for studying multitemperature flows of $CO_2$ in the shock layer in the flow past a flat plate [18], $N_2$/N flow around a wedge, and $O_2$/O flow across a one-dimensional shock with VT-exchange and dissociation [19]. However, up to now ANSYS Fluent has not been used for solving problems by the state-to-state approach because it takes into account deviations from equilibrium distributions for all internal degrees of freedom.

The present work is aimed at the development of a mathematical model for the description of binary mixture flows with allowance for vibrational and chemical kinetics and a code compatible with the basic solver of the chosen software package. The resultant numerical tool is verified by solving a problem of a gas flow across a one-dimensional shock wave. A two-dimensional flow around a cylinder is also simulated to test whether the tool is applicable for solving multidimensional problems.

## 1. Theoretical model

We consider a flow of a shock-heated $O_2(i)$/O mixture ($i$ is the vibrational level of molecules) with the following kinetic processes: VT(TV)-exchange of energy between translational and vibrational degrees of freedom

$$\mathrm{O}_2(i) + M \leftrightarrow \mathrm{O}_2(i \pm 1) + M, \quad M = \mathrm{O}_2, \mathrm{O}; \tag{2}$$

and dissociation reactions

$$\mathrm{O}_2(i) + M \rightarrow \mathrm{O} + \mathrm{O} + M, \quad M = \mathrm{O}_2, \mathrm{O}. \tag{3}$$

As the conversion of translational energy to non-excited vibrational degrees of freedom in a shock-heated gas dominate in the vibrational relaxation process, VV-exchange of vibrational energy between molecules was ignored in the present computations.

In view of the requirements of the basic solver and condition (1), the system of equations that describe the binary mixture flow includes equations for the mass fractions of the populations of vibrational levels of molecules $Y_i$, the mass fractions of atomic components $Y_{\text{a}}$, and also

equations for the macroscopic velocity **v** and translational temperature of the gas *T*. In the approximation of an inviscid non-heat-conducting gas, the system has the form

$$\partial\rho/\partial t + \nabla\cdot(\rho\mathbf{v}) = 0, \tag{4}$$

$$\partial\rho Y_i/\partial t + \nabla\cdot(\rho Y_i\mathbf{v}) = R_i, \quad i = 1,\ldots l, \tag{5}$$

$$\partial\rho Y_\mathrm{a}/\partial t + \nabla\cdot(\rho Y_\mathrm{a}\mathbf{v}) = R_\mathrm{a}, \tag{6}$$

$$\partial\rho\mathbf{v}/\partial t + \nabla\cdot(\rho\mathbf{v}\mathbf{v}) - \nabla p = 0, \tag{7}$$

$$\partial(\rho E)/\partial t + \nabla\cdot(\mathbf{v}(\rho E + p)) = S_h, \tag{8}$$

where $\rho$ and $p$ are the density and pressure of the mixture, $l$ is the number of excited levels of molecules, and $E = \frac{3}{2}\overline{R}_\mathrm{a}T\cdot Y_\mathrm{a} + \frac{5}{2}\overline{R}_\mathrm{m}T\cdot Y_\mathrm{m} + \frac{\mathrm{v}^2}{2}$ is the sum of the translational, rotational, and vibrational energies of the mixture per unit mass, where $Y_\mathrm{m} = \sum_{i=0}^{l} Y_i$ is the mass fraction of the molecular component of the mixture, and $\overline{R}_\mathrm{a}$ and $\overline{R}_\mathrm{m}$ are the specific gas constants of atomic and molecular components of the mixture. In the chosen software package, the system of the governing equations includes the continuity equation (4); for this reason, the kinetic equation for $Y_0$ was eliminated. The mass fraction of molecules of the zeroth level is calculated as $Y_0 = 1 - \sum_{i=1}^{l} Y_i - Y_\mathrm{a}$.

The right-hand sides of Eqs. (5)–(6) contain relaxation terms that describe the kinetic processes in the mixture. They have the form

$$R_i = R_i^{\mathrm{VTm}} + R_i^{\mathrm{VTa}} + R_i^{\mathrm{diss}} = \mathcal{M}_\mathrm{m}\left(\hat{R}_i^{\mathrm{VTm}} + \hat{R}_i^{\mathrm{VTa}} + \hat{R}_i^{\mathrm{diss}}\right), \tag{9}$$

$$R_\mathrm{a} = -2\mathcal{M}_\mathrm{a}\sum_{i}^{l}\hat{R}_i^{\mathrm{diss}}, \tag{10}$$

$$\hat{R}_i^{\mathrm{VTm}} = C_\mathrm{m}\sum_{i'=i\pm1}\left(C_{i'}k_{i'i}^\mathrm{m} - C_i k_{ii'}^\mathrm{m}\right), \tag{11}$$

$$\hat{R}_i^{\mathrm{VTa}} = C_\mathrm{a}\sum_{i'=i\pm1}\left(C_{i'}k_{i'i}^\mathrm{a} - C_i k_{ii'}^\mathrm{a}\right), \tag{12}$$

$$\hat{R}_i^{\mathrm{diss}} = -C_i(C_\mathrm{m}k_{i,\mathrm{diss}}^\mathrm{m} + C_\mathrm{a}k_{i,\mathrm{diss}}^\mathrm{a}), \tag{13}$$

where $\mathcal{M}_\mathrm{m}$ and $\mathcal{M}_\mathrm{a}$ are the molar weights of molecules and atoms in the mixture, $C_i$ is the molar concentration of molecules at the $i$th level, $C_\mathrm{m}$ and $C_\mathrm{a}$ are the molar concentrations of molecules and atoms, and $k_{ii'}^\mathrm{m}$, $k_{ii'}^\mathrm{a}$, $k_{i,\mathrm{diss}}^\mathrm{m}$, and $k_{i,\mathrm{diss}}^\mathrm{a}$ are the rate coefficients of energy exchange (2) and dissociation (3) in the case of collisions with molecules and atoms (marked by the subscripts "m" and "a", respectively).

The dissociation rate coefficients are found by using the Treanor–Marrone model [20], which was modified in [2] for the state-to-state approach:

$$k_{i,\mathrm{diss}}^{\mathrm{m,a}} = Z_i(T,U)k_{\mathrm{diss\text{-}eq}}^{\mathrm{m,a}}(T), \tag{14}$$

where $Z_i$ is the nonequilibrium factor, which has the form

$$Z_i(T,U) = \frac{Z^{\text{vibr}}(T)}{Z^{\text{vibr}}(-U)} \exp\left(\frac{\varepsilon_i}{k}\left(\frac{1}{T}+\frac{1}{U}\right)\right), \tag{15}$$

where $\varepsilon_i$ is the vibrational energy of the $i$th level of a molecule, $k$ is the Boltzmann constant, $U$ is the model parameter (in the present computations, we use $U = D/6k$, where $D = 8.197 \cdot 10^{-19}$ J is the dissociation energy), and $Z^{\text{vibr}}(T) = \sum_i \exp\left(-\varepsilon_i / kT\right)$ is the vibrational partition function. The equilibrium dissociation rate coefficient $k^{\text{m,a}}_{\text{diss-eq}}$ (m$^3$/s) is described by the Arrhenius formula

$$k^{\text{m,a}}_{\text{diss-eq}}(T) = AT^b \exp\left(-D/(kT)\right) \tag{16}$$

with the parameters $A = 5.33 \cdot 10^{-11}$ and $b = -1$ in the case of a collision with a molecule and $A = 1.5 \cdot 10^{-10}$ and $b = -1.05$ in the case of a collision with an atom [21]. The vibrational energy $\varepsilon_i$ is described by the harmonic oscillator model, and the number of excited levels for oxygen is $l$ = 25. The number of excited vibrational levels $l$ is found from the condition that the vibrational energy of the last level does not exceed the energy of dissociation of oxygen molecules.

The VT-exchange rate coefficients for the harmonic oscillator have the form

$$k^{\text{m,a}}_{ii'} = ik^{\text{m,a}}_{10}(T) \quad \text{for} \quad i' = i-1, \tag{17}$$

$$k^{\text{m,a}}_{ii'} = (i+1)k^{\text{m,a}}_{10}(T)\exp\left(-\frac{\theta_{\text{v}}}{T}\right) \quad \text{for} \quad i' = i+1, \tag{18}$$

where $\theta_{\text{v}}$ = 2267.5 K is the characteristic vibrational temperature of oxygen molecules, and $k^{\text{m,a}}_{10}(T)$ are the rate coefficients of the molecule transition from the 1st to the 0th vibrational level, which depend on the translational temperature of the gas and on the partner in the collision. The coefficients $k^{\text{m,a}}_{10}(T)$ are calculated in this work by the formulas of the SSH-theory [22, 23].

The right-hand side of Eq. (8) describes the change in the vibrational energy and the energy of mixture formulation as a result of processes (2)–(3). It can be written as

$$S_h = -\sum_i^l \frac{\varepsilon_i}{m_{\text{m}}} R_i - \frac{\varepsilon_{\text{a}}}{m_{\text{a}}} R_{\text{a}}, \tag{19}$$

where $\varepsilon_{\text{a}}$ is the standard state enthalpy of atoms, and $m_{\text{m}}$ and $m_{\text{a}}$ are the masses of oxygen molecules and atoms.

## 2. Implementation

The state-to-state description of nonequilibrium kinetics is modeled in the ANSYS Fluent software package in the following manner. Oxygen molecules located at different vibrational levels are simulated as independent components of the gas mixture (see Eq. (5)). The transitions to the upper and lower levels are interpreted by the solver as the chemical reactions

$$\text{O}_2(i) \xrightarrow{\hat{R}_i^{\text{VT,up}}} \text{O}_2(i+1), \tag{20}$$

$$\text{O}_2(i) \xrightarrow{\hat{R}_i^{\text{VT,down}}} \text{O}_2(i-1). \tag{21}$$

A total of 50 transitions between vibrational levels of molecular oxygen are considered. Energy exchange between vibrational and translational degrees of freedom in the case of a collision of an oxygen molecule located at the *i*th level with any other particle is simulated by analogy with chemical reactions. The standard state enthalpy $h_i^0$ equal to the vibrational energy of the level is determined for each vibrational level in the material properties of the solver. In this case, it is taken into account that the translational-rotational energy decreases by the difference in the energies between the neighboring vibrational states in the transition from the level *i* to the next (upper) level *i*+1 and increases by the same value in the transition from the upper to the lower level.

For a correct description of VT-exchange, the transition rates (20) and (21) have the form

$$\hat{R}_{\mathrm{i}}^{\mathrm{VT,up}} = C_{\mathrm{m}} C_i k_{i,i+1}^{\mathrm{m}} + C_{\mathrm{a}} C_i k_{i,i+1}^{\mathrm{a}}, \tag{22}$$

$$\hat{R}_i^{\mathrm{VT,down}} = C_{\mathrm{m}} C_i k_{i,i-1}^{\mathrm{m}} + C_{\mathrm{a}} C_i k_{i,i-1}^{\mathrm{a}}. \tag{23}$$

Relations (22) and (23) yield the absolute values of the relaxation terms, and the sign is determined by the solver with allowance for the stoichiometric coefficients of the reactions.

The energy exchange rate coefficients are described in the general case by a function that differs from the Arrhenius formula, which is a default formula of the solver for calculating the chemical reaction rate coefficients. Therefore, the VT-exchange rate coefficients are calculated by Eqs. (22) and (23) in the DEFINE_VR_RATE macros. In this case, the solver employs the user's code rather than the built-in default function.

Dissociation is modeled as a set of chemical reactions

$$\mathrm{O}_2(i) \xrightarrow{\hat{R}_i^{\mathrm{diss}}} \mathrm{O} + \mathrm{O}, \tag{24}$$

each describing decomposition of molecules located at the *i*th level into atoms. The probability of dissociation depends on the number of the vibrational level; correspondingly, 26 reactions are considered. The energy loss due to dissociation for the atomic species is taken into account with the use of the standard state enthalpy $h_{\mathrm{a}}^0 = \dfrac{\mathcal{M}_{\mathrm{a}}}{m_{\mathrm{m}}} \varepsilon_{\mathrm{a}}$ ($h_{\mathrm{a}}^0 = 2.4682 \cdot 10^8$ J/kmol for O).

The relaxation terms $\hat{R}_i^{\mathrm{diss}}$ are also calculated by means of a user-defined function.

In simulation of VT-transitions and dissociation, the particle *M* is eliminated from Eqs. (2) and (3) because it remains unchanged, but the rate coefficients of these processes are calculated with allowance for the presence of a partner in the collision. Such an approach allows the standard mechanism of the solver to be used for calculating the source terms in Eq. (5) in modeling chemically reacting flows; therefore, it is no longer necessary to implement these source terms in user-defined functions. It should be noted that writing VT-transitions in the form of Eqs. (20) and (21) and dissociation reactions in the form of Eq. (24) significantly reduces the computational expenses as compared to Eqs. (2) and (3). The point is that the rate of the transition from or to the *i*th level is calculated in Eqs. (20), (21), and (24) in one reaction, whereas Eqs. (2) and (3) require considering all particles *M* that may participate in collisions.

For the above-described chemical reactions, the source term implemented in the solver for taking into account the energy sources/drains due to chemical reactions has the form

$$S_{h,\mathrm{default}} = -\sum_{i=0}^{I} \frac{h_i^0}{\mathcal{M}_{\mathrm{m}}} \left( R_i^{\mathrm{VTm}} + R_i^{\mathrm{VTa}} \right) - \frac{h_{\mathrm{a}}^0}{\mathcal{M}_{\mathrm{a}}} R_{\mathrm{a}}, \tag{25}$$

and the source term necessary for calculating the flows on the basis of the state-to-state approach is

$$S_h = -\sum_{i=0}^{l} \frac{h_i^0}{\mathcal{M}_\mathrm{m}} \left( R_i^{\mathrm{VTm}} + R_i^{\mathrm{VTa}} \right) - \sum_{i=0}^{l} \frac{h_i^0}{\mathcal{M}_\mathrm{m}} R_i^{\mathrm{diss}} - \frac{h_\mathrm{a}^0}{\mathcal{M}_\mathrm{a}} R_\mathrm{a}, \tag{26}$$

where $h_\mathrm{a}^0 = \frac{\mathcal{M}_\mathrm{a}}{m_\mathrm{a}} \varepsilon_\mathrm{a}$ and $h_i^0 = \frac{\mathcal{M}_\mathrm{m}}{m_\mathrm{m}} \varepsilon_i$; the source term (25) is written in the default form in the solver for the above-given reactions, whereas the source term (26) is obtained from Eq. (19) with allowance for Eq. (9).

A comparison of Eqs. (25) and (26) shows that the term $-\sum_{i=0}^{l} \frac{h_i^0}{\mathcal{M}_i} R_i^{\mathrm{diss}}$ is ignored by the solver by default when the built-in mechanism of taking into account the energy source/drain is used. This term is calculated in the DEFINE_SOURCE macros and is then used as an additional source term in the right-hand side of Eq. (8).

Thus, the state-to-state approach for modeling inviscid non-heat-conducting gas flows with VT-exchange and dissociation is implemented. Flows of more complicated gas mixtures can be calculated in a similar manner. It should be noted that the above-described approach can be also used for other commercial software packages solving the same system of equations (4)–(8) of fluid dynamics.

### 3. Applications of the proposed approach

Three problems were considered:

I — VT (TV)-relaxation of pure oxygen behind the shock wave;

II — oxygen relaxation with VT (TV)-exchange and dissociation reactions behind the shock wave;

III — supersonic oxygen flow around a cylinder of radius $R$ = 1 cm with allowance for vibrational and chemical relaxation.

A two-dimensional rectangular domain is constructed for simulating the flow across a one-dimensional shock wave because the chosen software package is not designed for solving one-dimensional problems. Symmetry conditions are applied on the upper and lower boundaries, and two cells are constructed between them. The freestream (pressure-far-field) condition is set on the left boundary, and the pressure calculated at the end of the relaxation region is applied at the right (outlet) boundary (pressure-outlet boundary condition). A uniform structured rectangular grid is constructed in the computational domain with 500 cells between the left and right boundaries. The distance from the left to the right boundary is set to be 0.12 m.

A discontinuous solution is considered as the initial condition. The free-stream conditions are imposed ahead of the discontinuity, and the equilibrium values at the end of the relaxation region are set behind the discontinuity. These initial conditions are defined in the DEFINE_INIT macros. The free-stream conditions are chosen to be consistent with one of the experiments [24]: $\mathrm{M}_0$ = 9.3, $T_0$ = 299 K, and $p_0$ = 266.6 Pa, where $\mathrm{M}_0$, $T_0$, and $p_0$ are the Mach number, translational-rotational temperature, and static pressure, respectively.

The mixture is initially assumed to consist of molecular oxygen only, and the populations of the vibrational levels are assumed to have the Boltzmann distributions with a prescribed gas temperature $T_0$:

$$Y_i^B = \frac{Y_\mathrm{m}}{Z^{\mathrm{vibr}}(T_0)} \exp\left( -\frac{\varepsilon_i}{kT_0} \right), \tag{27}$$

where $Z^{\mathrm{vibr}}(T_0) = \sum_{i=0}^{l} \exp\left( -\frac{\varepsilon_i}{kT_0} \right)$.

The calculations are performed with the use of a density-based solver designed for modeling high-velocity compressible flows with a second-order implicit upwind scheme. The fluxes through the control volume faces are calculated with the AUSM solver [25].

For computing the flow around the cylinder, we constructed a computational domain around one quarter of the cylinder. A structured grid with 50×40 cells is constructed in this computational domain. The initial condition is a uniform supersonic flow with freestream parameters. The left boundary is subjected to the freestream conditions (pressure-far-field in the terminology of the chosen software package). By virtue of problem symmetry, the symmetric condition is set on the lower boundary. The cylinder wall is subjected to the condition of an inviscid wall, i.e., the boundary layer is ignored. As a supersonic flow is formed at the right (outlet) boundary, all variables are extrapolated from the computational domain (pressure-outlet boundary condition).

The results computed by the proposed numerical tool are compared with the flow parameters calculated in the shock-fitting formulation, which implies that the shock wave consists of a narrow shock front and an extended relaxation region. Only the fast processes (1) occur inside the shock front, whereas the chemical composition of the mixture and the distribution over the vibrational levels are unchanged. The problem solution procedure consists of two stages: finding the gas parameters immediately behind the shock front (they can be obtained from the Rankine–Hugoniot relations) and numerical integration of system (4)–(8) rewritten for a steady one-dimensional flow with the data obtained at the beginning of the relaxation region. In such a formulation, the problem was previously solved by one of the authors of the present paper (see, e.g., [6]).

Figure 1 shows the behavior of the translational temperature and mass fractions of individual vibrational levels with distance from the shock front, which were calculated in modeling the flow across the shock wave for pure oxygen with allowance for VT (TV)-relaxation (problem I). The gas parameters obtained in the present work and in shock-fitting computations are compared in the figure. It is seen that the gas temperature decreases with increasing distance $x$, and the number of molecules at the non-zero level increases owing to TV-activation of the gas. As the distance from the shock front increases, the gas parameters approach constant values corresponding to thermal equilibrium.

The differences between the parameters predicted by two numerical methods are caused by the differences in the numerical approaches to solving the problem. In the shock-fitting computations, the translational-rotational temperature changes instantaneously, whereas the shock wave in the shock-capturing computations is smeared over two computational cells. As a result of such a numerical effect (artifact), the energy exchange begins earlier than in the shock-capturing computations. Because of the earlier TV-transitions, the translational-rotational temperature decreases, leading to differences in the level populations (see Fig. 2*b*).

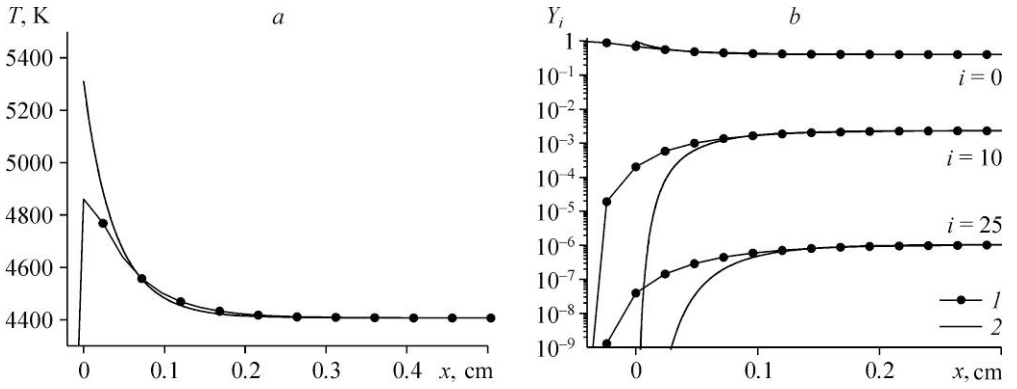


*Fig. 1*. Translational-rotational temperature of the gas (*a*) and mass fractions of vibrational level populations (*b*) as functions of $x$.

*1* — results computed by the proposed numerical tool,
*2* — results of shock-fitting computations.

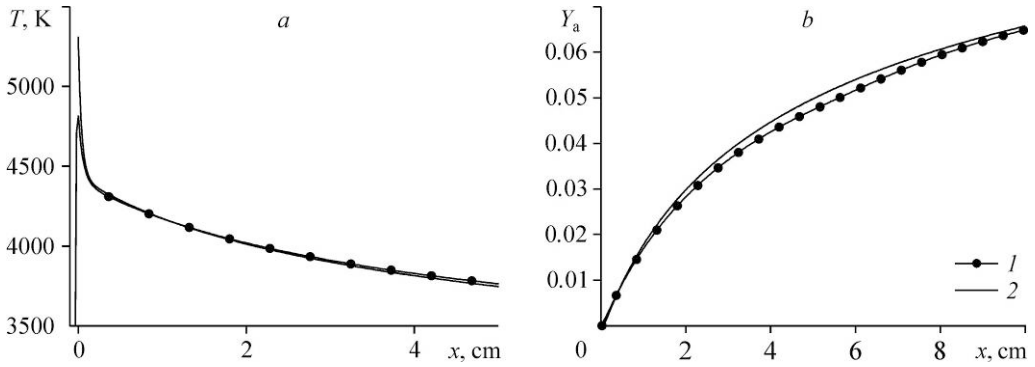


*Fig. 2*. Translational-rotational temperature of the gas mixture (*a*) and mass fraction of atomic oxygen (*b*) as functions of *x*.

See the notations in Fig. 1.

Numerical oscillations on shock waves, which are typical of inviscid numerical solutions in the chosen software package, should be noted. Despite a moderate amplitude of these numerical oscillations, they may exert a certain effect on the distributions of the populations of the last levels (their values are very small). At $x > 0.1$ cm, the flow parameters predicted by two methods completely coincide, which confirms that the implementation considered in the previous paragraph is correct.

The macroparameters calculated by two numerical methods for the problem formulation with vibrational and chemical relaxation (problem II) are compared in Figs. 2 and 3. It is seen that the values are close to each other. The difference at the beginning of the relaxation region at $x = 0$ is also caused by the difference in the numerical approaches to solving the problem (shock-fitting and shock-capturing approaches). The mechanism of these differences completely coincides with that described for problem I; however, here we should note the dissociation process, which affects the changes in the populations $Y_i$ at $i > 0$ (see Fig. 3*a*): first they increase owing to vibrational excitation of molecules, and then decrease owing to dissociation.

For validation of the proposed model, the computed vibrational temperature is compared (see Fig. 3*b*) with the corresponding temperature measured in the experiment [24]. The computation is performed for the molecule distributions over the vibrational levels being far from equilibrium. As a result, vibrational temperature determination in the state-to-state approach is not obvious. The value of this temperature is estimated by the relation for the temperature of

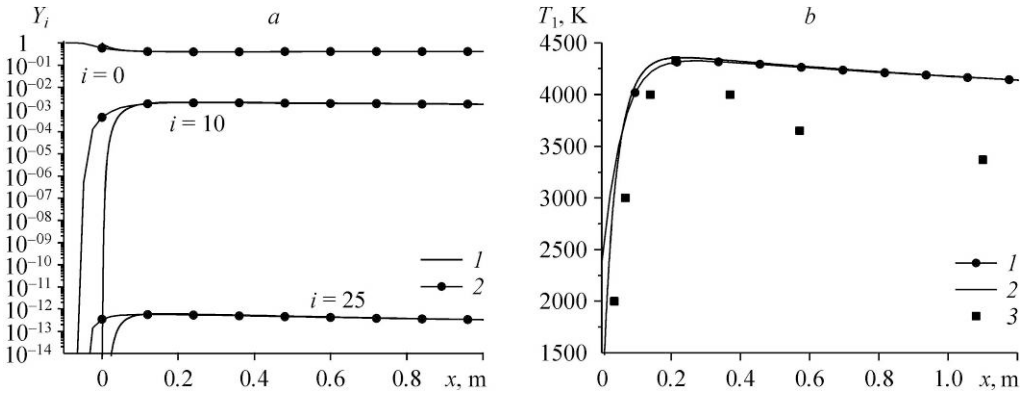


*Fig. 3*. Mass fractions of the populations of individual vibrational levels of molecules (*a*) and vibrational temperature (*b*) as functions of *x*.

*1* — results computed by the proposed numerical tool, *2* — results of shock-fitting computations, *3* — experimental data.

the first vibrational level proposed in the multitemperature approach based on using quasi-steady distributions and associated with the total number of vibrational quanta. Thus, the vibrational temperature $T_1$ for the state-to-state approach is calculated by the relation $T_1 = \varepsilon_1 / k \ln(Y_0 / Y_1)$.

A comparison with the experiment (see Fig. 3*b*) under the considered conditions reveals good agreement in the gas excitation region; however, the difference in the deactivation region with increasing $x$ increases and reaches 23 %. Nevertheless, the behavior of the numerical and experimental curves behind the vibrational temperature peak is qualitatively similar. The difference of the numerical results from the experimental data can be related to the choice of the models used for calculating the rate coefficients of the kinetic processes and requires additional investigations. Such a study was previously performed in [26] within the framework of the multitemperature kinetic approach and in [27] by the direct simulation Monte Carlo method.

Figures 4 and 5 show the flow fields around the cylinder, which were obtained in the computations performed with the proposed numerical tool (problem III). The bow shock wave upstream of the cylinder is clearly seen in Fig. 4*a*. In the plane of symmetry, it is actually a normal shock with a subsonic flow behind it. However, with distance from the plane of symmetry, the bow shock wave becomes curved, resulting in a decrease in the Mach number normal to the wave. This curvature reduces the shock intensity, and a supersonic flow starts to form behind the wave. The black solid curve in the flow field is the sonic line bounding the subsonic region. A supersonic flow is formed at the right (outlet) boundary, which confirms the correctness of extrapolation of all variables from the computational domain. Figure 4*b* shows the translational-rotational temperature field, where the streamlines are indicated by black arrows. There is a peak of the translational-rotational temperature immediately behind the bow shock wave in the plane of symmetry, which is induced by the greatest intensity of the shock wave. Then the temperature decreases owing to TV-transitions and dissociation. The translational-rotational temperature decreases with distance from the plane of symmetry owing to lower shock wave intensity.

Figure 5 shows the mass fractions of atoms and molecules at the 10th vibrational level. It is clearly seen that the mass fraction of atoms increases (Fig. 5*a*) from 0 in the free stream to 0.0185 in the region behind the cylinder. This is related to the finite rates of dissociation and TV-transitions. The populations of non-zero levels behave nonmonotonically, increasing due to TV-exchange and decreasing due to dissociation, as is seen from Fig. 5*b*. Because of the dissociation delay, the maximum of the mass fraction of the atomic component is observed only near the cylinder.

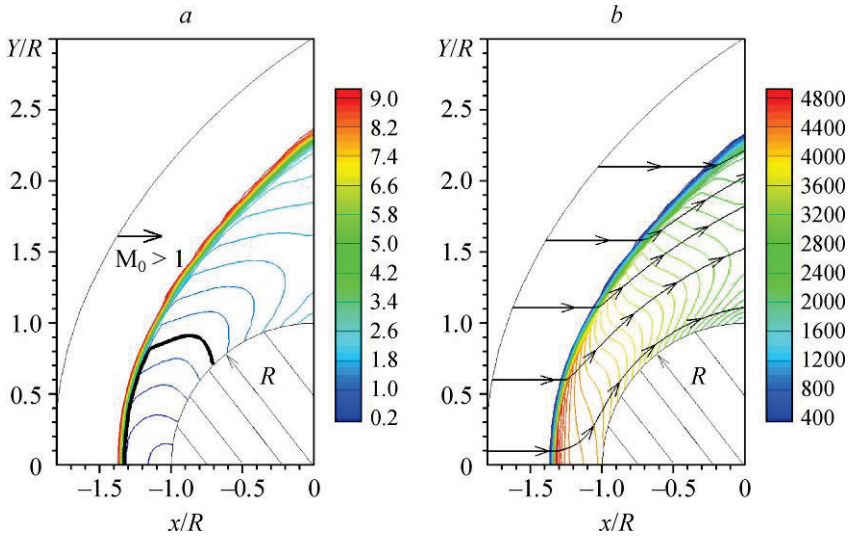


*Fig. 4.* Distributions of the Mach number (*a*) and translational-rotational temperature of the gas (*b*).

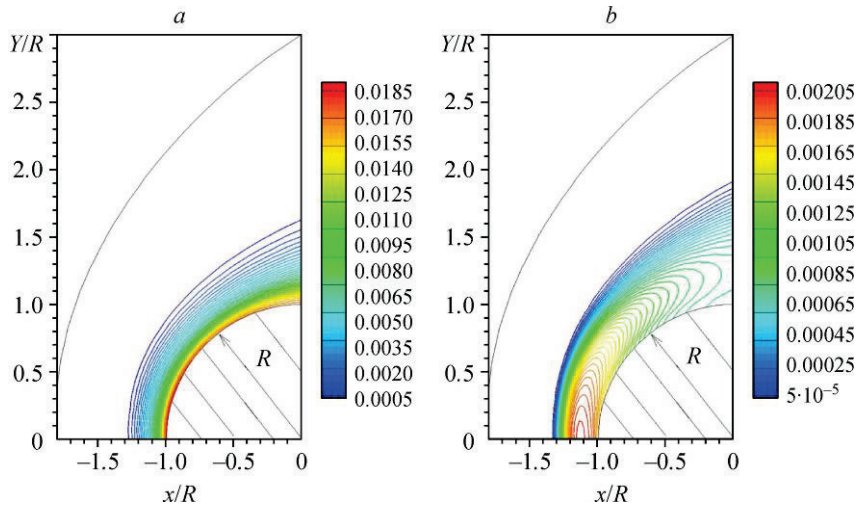


*Fig. 5*. Distributions of the mass fractions of atoms (*a*) and molecules at the 10th vibrational level (*b*).

As a whole, it can be noted that the numerical tool proposed in the present paper can be used for further numerical investigations of high-enthalpy gas flows by using the state-to-state approach.

## Conclusions

A method of computing nonequilibrium flows based on the state-to-state approach is proposed. The method is implemented in the ANSYS Fluent software package and includes a user-defined code for calculating the rate coefficients of VT (TV)-transitions, dissociation, and an additional source term in the equation of conservation of translational-rotational energy for a correct description of the state-to-state kinetics.

Verification of the proposed numerical tool is performed. For this purpose, the flow across the shock wave is calculated, and the resultant parameters are compared with the numerical solution obtained by the authors' code. The numerical data are found to agree well. The proposed numerical tool is tested by means of solving the classical problem of the flow around a cylinder. The presented results lead to a conclusion that the proposed numerical tool can be used in the future for calculating more complicated problems: studying viscous heat-conducting flows with new algorithms for computing transport coefficients.

The computed distributions of the vibrational temperature of molecular oxygen behind the normal shock are compared with experimentally measured values. The vibrational temperature peaks are found to agree well, whereas there are certain differences in the numerical and experimental data behind these peaks, which are caused by the differences in the energy exchange and dissociation models used in the study. Various models of the state-to-state kinetics will be validated through comparisons with experimental data for various one-dimensional, two-dimensional, and three-dimensional flows with the use of the technique proposed and tested in this paper.

## References

1. **R. Brun,** Introduction to Reactive Gas Dynamics, Oxford University Press, 2009.
2. **E. Nagnibeda and E. Kustova,** Nonequilibrium Reacting Gas Flows. Kinetic Theory of Transport and Relaxation Processes, Springer, Berlin, 2009.
3. **F. Lordet, J. Meolans, A. Chauvin, and R. Brun,** Nonequilibrium vibration-dissociation phenomena behind a propagating shock wave: vibrational population calculation, Shock Waves, 1995, Vol. 4, P. 299–312.

4. **I. Adamovich, S. Macheret, J. Rich, and C. Treanor,** Vibrational relaxation and dissociation behind shock waves, AIAA J., 1995, Vol. 33, No. 6, P. 1064–1075.
5. **E. Kustova and E. Nagnibeda,** The influence of the state-to-state distributions behind shock wave on the dissociation rates, in: Proc. 22nd Int. Symp. on Shock Waves, 2000, Vol. 1, P. 783–788.
6. **O. Kunova, E. Kustova, M. Mekhonoshina, and E. Nagnibeda,** Non-equilibrium kinetics, diffusion and heat transfer in shock heated flows of $N_2$/N and $O_2$/O mixtures, Chemical Phys., 2015, Vol. 463, P. 70–81.
7. **B. Shizgal and F. Lordet,** Vibrational nonequilibrium in a supersonic expansion with reactions: Application to $O_2$-O, J. Chem. Phys., 1996, Vol. 104, No. 10, P. 3579–3597.
8. **G. Colonna, M. Tuttafesta, M. Capitelli, and D. Giordano,** Influence of $O_2(v)$+N=NO+O on NO formation in one-dimensional air nozzle flow, J. Thermophysics and Heat Transfer, 2000, Vol. 14, No. 3, P. 455–456.
9. **E. Kustova, E. Nagnibeda, T. Alexandrova, and A. Chikhaoui,** On the non-equilibrium kinetics and heat transfer in nozzle flows, Chem. Phys., 2002, Vol. 276, P. 139–154.
10. **I. Armenise, M. Capitelli, and C. Gorse,** Nonequilibrium vibrational kinetics in the boundary layer of re-entering bodies, J. Thermophysics and Heat Transfer, 1996, Vol. 10, No. 3, P. 397–405.
11. **I. Armenise, F. Esposito, and M. Capitelli,** Dissociation-recombination models in hypersonic boundary layer, Chem. Phys., 2007, Vol. 336, P. 83–90.
12. **E. Josyula, E. Kustova, P. Vedula, and J.M. Burt,** Influence of state-to-state transport coefficients on surface heat transfer in hypersonic flows, in: Proc. 52nd Aerospace Sci. Meeting, AIAA paper No. 2014–0864, 2014.
13. **E. Josyula, J.M. Burt, E. Kustova, P. Vedula, and M. Mekhonoshina,** State-to-state kinetic modeling of dissociating and radiating hypersonic flows, in: Proc. 53rd AIAA Aerospace Sci. Meeting, AIAA paper No. 2015–0475, 2015.
14. **E. Kustova and E. Nagnibeda,** Transport properties of a reacting gas mixture with strong vibrational and chemical nonequilibrium, Chem. Phys., 1998, Vol. 233, P. 57–75.
15. **E. Kustova and G. Kremer,** Chemical reaction rates and non-equilibrium pressure of reacting gas mixtures in the state-to-state approach, Chem. Phys., 2014, Vol. 445, P. 82–94.
16. **Yu.P. Gounko and I.I. Mazhul,** Numerical investigation of flow over two sweepback wedges at M = 4 and 6, Thermophysics and Aeromechanics, 2013, Vol. 20, No. 2, P. 179–193.
17. **Yu. P. Gounko and I.I. Mazhul,** Numerical modeling of the conditions for realization of flow regimes in supersonic axisymmetric conical inlets of internal compression, Thermophysics and Aeromechanics, 2015, Vol. 22, No. 5, P. 545–558.
18. **S.V. Kirilovskiy, A.A. Maslov, T.V. Poplavskaya, and I.S. Tsyryul'nikov,** Influence of vibrational relaxation on perturbations in a shock layer on a plate, Techn. Phys, 2015, Vol. 60, No. 5, P. 645–655.
19. **G.V. Shoev, Ye.A. Bondar, G.P. Oblapenko, and E.V. Kustova,** Development and testing of a numerical simulation method for thermally nonequilibrium dissociating flows in ANSYS Fluent, Thermophysics and Aeromechanics, 2016, Vol. 23, No. 2, P. 151–163.
20. **P. Marrone and C. Treanor,** Chemical relaxation with preferential dissociation from excited vibrational levels, Phys. Fluids, 1963, Vol. 6, P. 1215–1221.
21. **T.J. Scanlon, C. White, M.K. Borg, R.C. Palharini, E. Farbar, I.D. Boyd, and R.E. Brown,** Open-source direct simulation Monte Carlo chemistry modeling for hypersonic flows, AIAA J., 2015, Vol. 53, No. 6, P. 1670–1680.
22. **R. Schwartz, Z. Slawsky, and K. Herzfeld,** Calculation of vibrational relaxation times in gases, J. Chem. Phys., 1952, Vol. 20, P. 1591–1599.
23. **G. Chernyi, S. Losev, S. Macheret, and B. Potapkin,** Physical and Chemical Processes in Gas Dynamics. Vol. 1, American Institute of Aeronautics and Astronautics, 2002.
24. **L.B. Ibraguimova, A.L. Sergievskaya, V.Y. Levashov, O.P. Shatalov, Y.V. Tunik, and I.E. Zabelinskii,** Investigation of oxygen dissociation and vibrational relaxation at temperatures 4000–10800 K, J. Chem. Phys., 2013, Vol. 139, P. 034317-1–034317-10.
25. **M.S. Liou and C.J. Steffen Jr.,** A new flux splitting scheme, J. Comput. Phys., 1993, Vol. 107, Iss. 1, P. 23–39.
26. **E. Kustova, E. Nagnibeda, G. Oblapenko, A. Savelev, and I. Sharafutdinov,** Advanced models for vibrational–chemical coupling in multi-temperature flows, Chem. Phys., 2016, Vol. 464, P. 1–13.
27. **I. Wysong, S. Gimelshein, Ye. Bondar, and M. Ivanov,** Comparison of direct simulation Monte Carlo chemistry and vibrational models applied to oxygen shock measurements, Phys. Fluids, 2014, Vol. 26, P. 043101-1–043101-15.